Codebook beam characterization approach with dual band for 6G 140 GHz, 300 GHz UE array

Rajesh Vedala, Tom Daniel
Verizon Wireless, USA

***Abstract*—Experimental results from 5G FR2 CATR OTA measurement practices, this paper outlines beam codebook design for a mobile UE operating at 140 GHz and 300 GHz. The modeled UE uses two dual band antenna modules, one on the rear and one on the side edge. Each module contains a shared 2×5 array with 0.5 mm element spacing, approximately half a wavelength at 300 GHz. The modem controls beam steering and selects the active module. Under the assumed element pattern model, beamwidths are 139.3° at 140 GHz and 65° at 300 GHz, with estimated peak element gains of 3.28 dBi and 9.90 dBi, respectively. Three methods are compared using the spherical EIRP CDF: (a) a single beam per module with jointly optimized steering, (b), a dense uniform codebook with jointly optimized scan ranges and beam overlap, and (c) a gap directed codebook that adds beams to improve the current 10th percentile EIRP. At 140 GHz, the gap directed method achieves 17.57 dBm using 30 beams, compared with 17.51 dBm using 110 dense codebook beams. At 300 GHz, it achieves −0.32 dBm using 30 beams, compared with −0.15 dBm using 486 beams. These results show that the gap directed method approaches dense codebook performance at the 10th percentile while reducing beam count by approximately $3.7\times$ and $16.2\times$ at the two bands.**

***Index Terms*—6G, subTHz, 5G FR2, user equipment, dual band array, shared element, beam codebook, OTA testing, EIRP, spherical coverage.**

I. Introduction

Experiments from 5G FR2 UE testing indicate that strong peak EIRP alone does not ensure good coverage in every direction. CATR measurements record EIRP across the sphere and summarize its distribution using a cumulative distribution function (CDF). Lower percentiles point performance in weaker directions, where limited beam coverage or blockage can reduce the available link margin.

This paper applies the evaluation approach to a two module UE operating at 140 GHz and 300 GHz. Each module contains a shared dual band 2×5 uniform rectangular array with the 0.5 mm element spacing is approx half a wavelength at 300 GHz but only 0.233 wavelengths at 140 GHz, giving the array different beam widths and steering responses at the two bands, further the element patterns are modeled using an assumed beam width scaling with wavelength and corresponding peak gain estimates. The validation process explains how beam codebook design can improve coverage in weaker directions while limiting the number of beam states. Three methods are compared: one jointly optimized beam per module, a dense uniform codebook, and a gap directed codebook that adds beams to improve the current 10th percentile EIRP. Each method is evaluated over 6000 directions distributed approx uniformly across the sphere, using the same module geometry and fixed input power per element within each band, this work makes three contributions. First, it defines a shared array model with explicit element pattern assumptions at both frequencies. Second, it jointly searches the codebook parameters of the two modules within each band, allowing their coverage regions to complement one another. Third, it quantifies the tradeoff between beam count and spherical coverage through a comparison of the three methods under the same conditions. The gap directed method approaches the dense codebook's 10th percentile EIRP using 30 beams per band, compared with 110 beams at 140 GHz and 486 beams at 300 GHz.

Performance is examined at the 10th, 20th, 30th, 50th, and 80th percentiles. The weaker lower percentile results at 300 GHz reflect the assumed element patterns, array response, and module orientations in this model.

II. Related Work

The element pattern formulation used in this study is adapted from 3GPP TR 38.901 [1]. Its application at 140 GHz and 300 GHz is a modeling extension beyond the standard's stated frequency range. Research from NYU WIRELESS examines the feasibility of outdoor communication link above 100 GHz and the role of antenna arrays and beamforming [2]. Measurement systems and campaigns near 140 GHz provide further context for propagation and attenuation at these frequencies [3], [4].

Several industry demonstrations illustrate progress in sub THz hardware and measurement systems from the gNB view point. Rohde & Schwarz has reported an outdoor 300 GHz duplex link over 645 m at 12.6 Gbps [5], together with a photonic measurement system operating beyond 500 GHz [6]. Keysight has developed a testbed covering 110 GHz to 220 GHz for waveform validation [7] and reported a 100 Gbps link with the UK's National Physical Laboratory and the University of Surrey [8]. Fraunhofer HHI also operates an outdoor THz wireless testbed integrated with optical fiber infrastructure in Berlin [9]. These developments demonstrate progress in radio front ends, antenna systems, and channel measurements. Applying this technology to mobile UEs introduces additional constraints on module size, transmit power, power consumption, and spherical coverage. The present study addresses these UE requirements by comparing beam codebook designs for a compact device with a limited number of antenna modules.

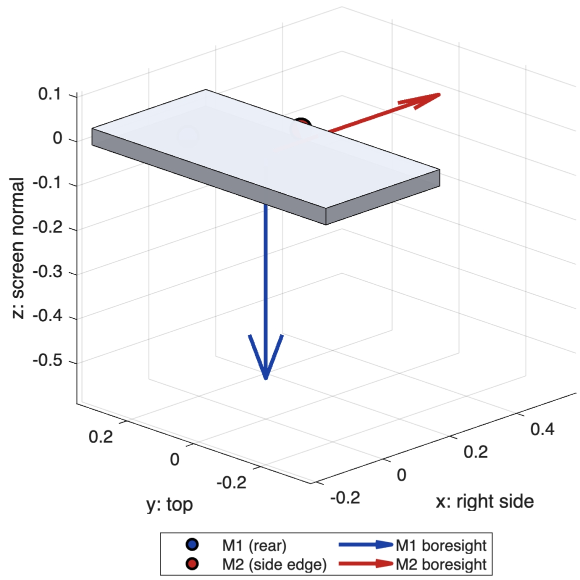

Fig. 1. Two module UE geometry. M1 is rear placed with boresight along $+\hat{z}$, and M2 is placed on the right edge with boresight along $+\hat{x}$. Each module contains a shared dual band 2×5 array.

III. System Model

A. Shared Dual Band Array and Module Geometry

Each UE module has a shared dual band 2×5 uniform rectangular array, with five elements along its long axis and two along its short axis. The element spacing is

$$d = \frac{c}{2f_{300}} \approx 0.5\,\mathrm{mm}, \tag{1}$$

corresponding to half a wavelength at 300 GHz and approximately 0.233 wavelengths at 140 GHz. This spacing is selected to control grating lobes at the higher band. Steering to the max limits with additional checking because of half wavelength spacing and to produce equivalent array factor in opposite steering directions.

Module 1 (M1) is placed on the rear, with its outward normal along $+\hat{z}$, long axis along $\hat{y}$, and short axis along $\hat{x}$. Module 2 (M2) is placed on the right edge, with its outward normal along $+\hat{x}$, long axis along $\hat{z}$, and short axis along $\hat{y}$.

For each observation direction $\hat{u}$, the modem selects the module and beam that provide the highest EIRP:

$$\mathrm{EIRP}(\hat{u}) = \max_{m\in\{1,2\}} \mathrm{EIRP}_{\mathrm{M}m}(\hat{u}), \tag{2}$$

where each module's EIRP is evaluated using its best available beam ID. Only one module serves a direction at a time.

The model assumes far field operation in free space and excludes chassis interaction, coupling, and user blockage. Under these assumptions, moving a module without changing its orientation leaves the calculated coverage CDF unchanged.

As shown in Fig. 1, the module boresights are 90° apart. They provide coverage regions that may overlap, with switched selection choosing the stronger available response in each direction.

B. Dual Band Element Pattern

The element pattern uses the angular attenuation form of 3GPP TR 38.901 Table 7.3-1 as a modeling approx. Gain decreases away from boresight in the horizontal and vertical planes, with the combined attenuation capped at 30 dB. [10], [11] Peak gain is estimated separately from the approximate directivity relation, assuming ideal radiation efficiency:

$$G_{\max} \approx 10\log_{10}\left(\frac{41253}{\theta_{3\mathrm{dB,H}}\theta_{3\mathrm{dB,V}}}\right), \tag{3}$$

where both beamwidths are expressed in degrees. For equal horizontal and vertical beamwidths, this simplifies to

$$G_{\max} \approx 10\log_{10}\left(\frac{41253}{\theta_{3\mathrm{dB}}^2}\right). \tag{4}$$

The modeling is an approx, shared physical radiating aperture whose beamwidth scales approximately with wavelength. Setting the beamwidth at 300 GHz to 65° gives

$$\theta_{3\mathrm{dB},140} \approx 65^\circ \frac{300}{140} = 139.3^\circ. \tag{5}$$

The corresponding peak gain estimates are 9.90 dBi at 300 GHz and 3.28 dBi at 140 GHz. Under this assumption, the lower band has a broader, less directive element pattern.

These values are analytical estimates of antenna characteristics. The beamwidth approximation is particularly limited for broad patterns. A practical dual band element supporting different current distributions at each frequency, so its beamwidth and gain may differ from these estimates. Each band therefore uses a separate beam codebook, described in Sec. IV, while practical implementation requires band specific calibration /phase array / Beam IDs.

Input power per element is assumed to be 4 dBm at 140 GHz and 0 dBm at 300 GHz. For ten equally powered elements, the total input power is 10 dB higher than for one element. Under an ideal array approximation, coherent excitation can provide a further 10 dB increase in directivity. These are separate contributions to EIRP, not a 20 dB directivity gain. The actual directivity depends on element spacing, radiation patterns, steering, and coupling, and possibly integrating the Beam IDs combined radiation pattern.

C. Physical Steering Limit

In this array model, steering depends on the sine of the commanded angle, which ranges from -1 to $+1$. Different angles can therefore produce identical element phase settings. For example, $\sin(125^\circ) = \sin(55^\circ)$, so both commands produce the same radiation pattern when the element pattern is held fixed. Similarly, the commands of $+91^\circ$ and -91° are equivalent to $+89^\circ$ and -89°, respectively. Steering beyond $\pm 90^\circ$ therefore does not create additional beam patterns or extend the spherical coverage in this model.

IV. Beam Codebook Methodology

All three methods use the same physical layout and system model described in Sec. III. Coverage is evaluated using the CDF, $\mathrm{EIRP}(\hat{u})$, across sampled spherical directions. Results are reported at the 10th, 20th, 30th, 50th, 80th, and 100th percentiles. Lower percentiles describe coverage in weaker directions, while the 100th percentile represents the highest sampled EIRP, which need not occur at module boresight. Each method is evaluated separately at the two frequency bands.

1) Method (i): Jointly Optimized Single Beam: Each module uses one beam, defined by a fixed phase gradient across its ten elements. The long and short axis steering angles of both modules are searched jointly using a coarse 10° grid. Each combination is scored by the combined 10th percentile EIRP, followed by a 2° local refinement around the best coarse configuration. Joint selection accounts for how the two modules complement each other. Optimizing each module independently does not necessarily maximize their combined coverage, because the preferred steering angles depend on the directions already served by the other module. The selected configuration is the best found within the evaluated search grids.

2) Method (ii): Dense Uniform Codebook: Each module uses a grid of beams with spacing determined by a selected crossover level between neighboring beams. The evaluated levels are 3 dB, 2 dB, 1.5 dB, 1 dB, and 0.5 dB below the beam peak. Smaller crossover losses require closer beam spacing and generally increase the beam count.

Spacing is calculated numerically for the five element long axis and the two element short axis. The resulting beam grid spans the selected scan range on each axis. Coverage is calculated by selecting the strongest available beam across both modules in each direction. Each module has $9 \times 9 \times 5 = 405$ candidate codebook configurations, covering nine long axis scan widths, nine short axis scan widths, and five crossover levels. All 405×405 module pairings are evaluated, and the pairing with the highest combined 10th percentile EIRP is selected. Thus, scan range and beam overlap are optimized jointly for the two modules.

3) Method (iii): Gap Directed Adaptive Codebook: This method builds the codebook one beam at a time from a shared candidate pool containing steering settings for both modules. At each step, every remaining candidate is temporarily added to the selected codebook, and the resulting 10th percentile EIRP is calculated. The candidate producing the highest score is retained, and the process repeats until the beam budget is reached. The selection process of aiming fo higher power beams, its Beam ID targets improvements in lower percentile coverage, including weak regions between the modules' coverage areas. Unlike uniform placement, it allocates beams according to their contribution to the combined spherical coverage metric.

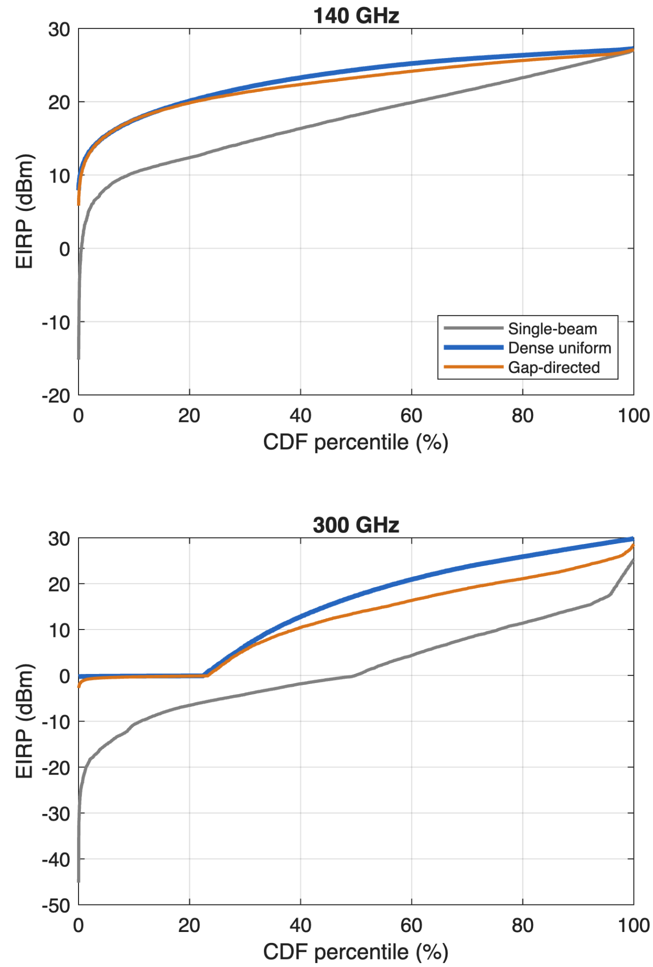

Fig. 2. Combined M1+M2 coverage CDF, all three methods, both bands. The single beam floor sits well below both multi beam method at every percentile; dense uniform and gap directed are close through the low to mid percentiles and separate above roughly the 30th.

TABLE I
140 GHz: combined M1+M2 EIRP percentiles (dBm) by method

Tier	Beams	p10	p20	p30	p50	p80	p100
(i) Singlebeam	2	10.34	12.37	14.44	18.18	23.29	27.07
(ii) Dense uniform	110	17.51	20.10	21.92	24.35	26.34	27.27
(iii) Gapdirected	30	17.57	19.85	21.29	23.28	25.62	27.14

V. Results

Table I and Table II report the full percentile tables for all three codebook beam methods at 140 GHz and 300 GHz, plotted in full in Fig. 2. In both tables, "beams" is the total across both antenna modules.

Fig. 3 indicates multiple nulls for 300 GHz and is directly a large deadzone, it is the direct visual signature of the element asymmetry from Sec. III B a resonant, directive element necessarily has a real off boresight roll off, a narrow region with slightly less power around 15 to 10dBm for 10th and 20th percentile at 140GHz spherical coverage.

Three findings follow from these tables.

TABLE II
300 GHz: COMBINED M1+M2 EIRP PERCENTILES (DBM) BY METHOD

Tier	Beams	p10	p20	p30	p50	p80	p100
(i) Singlebeam	2	10.71	6.53	4.13	0.02	11.39	25.22
(ii) Dense uniform	486	0.15	0.11	6.44	17.38	25.88	29.88
(iii) Gapdirected	30	0.32	0.15	5.51	13.62	21.09	28.62

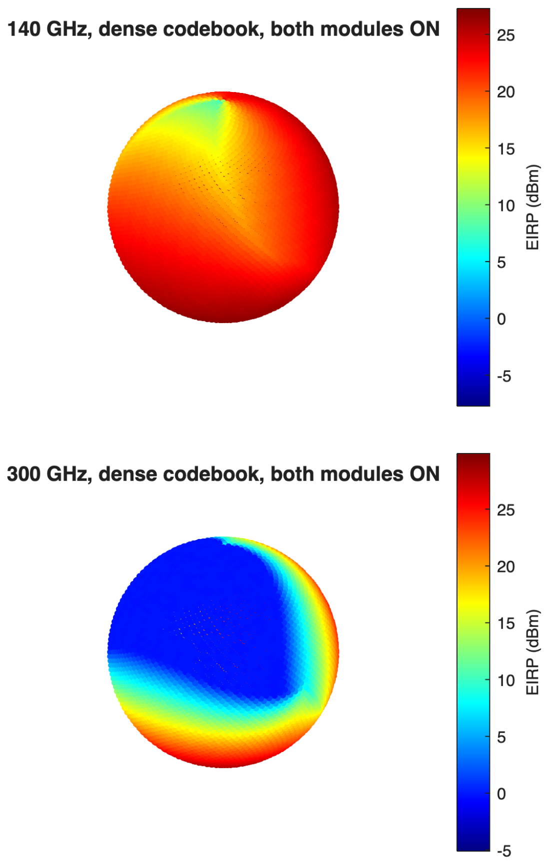

Fig. 3. Full sphere EIRP for the dense uniform codebook, both modules ON. 140 GHz's spherical coverage with minimal nulls ; 300 GHz's highly directed energy with lot of null region even with 486 beams.

Beam diversity improves spherical coverage. Moving from method (i) to method (ii) increases the 10th percentile EIRP by 7.17 dB at 140 GHz and 10.56 dB at 300 GHz, without changing the input power per element. The improvement therefore comes from selecting among additional steered beams. The larger improvement at 300 GHz reflects the narrower modeled patterns, which provide stronger directional gain but less angular coverage with a single beam. An additional module with a complementary orientation could help overcome the nulls.

Denser uniform grids provide diminishing returns. At 300 GHz, reducing the crossover loss from 3 dB to 0.5 dB increases the beam count from 66 to 486, approx 7.4 times as many beams. However, the 10th percentile EIRP improves by only 0.34 dB, from −0.49 dBm to −0.15 dBm. This indicates limited additional benefit at the selected percentile despite the substantial increase in beam count.

Gap directed placement reduces beam count. Using 30 beams per band, the gap directed method slightly exceeds the dense codebook's 10th percentile EIRP at 140 GHz and falls only 0.17 dB below it at 300 GHz. The corresponding dense beam codebook uses 110 and 486 beams, respectively. However, the dense codebook performs better at higher percentiles (directivity), illustrating the tradeoff between beam count, lower percentile coverage, and performance across the wider sphere.

VI. Design Precautions

1) **Dual band element spacing:** Select $d \leq \lambda_{\text{high}}/2$ using the highest operating frequency to control grating lobes.
2) **Steering range:** Restrict commands to $\pm 90^\circ$ within this model and use physically valid planar array steering combinations (in case of antenna placements in edges). Larger angles repeat existing phase settings rather than extend coverage.
3) **Beam count:** Balance beam overlap against diminishing improvements in the target CDF percentile. Further coverage gains may require measured codebook calibration, revised module orientations, or an additional module.

VII. Conclusion and Future Work

For the modeled two module UE, beam codebook design improves lower percentile spherical coverage at 140 GHz and 300 GHz without increasing input power per element. The gap directed method achieves similar 10th percentile EIRP with 30 beams per band, compared with 110 and 486 beams for the dense codebooks, respectively. These results demonstrate beam count savings, but do not establish that all coverage nulls are eliminated. Future work can examine third module placement orientation and its improved Spherical coverage with reduced nulls.

Acknowledgment

The author Rajesh thank Hrant Vardanyan for continued support and technical guidance, and Palak Kapoor of NIT-Waranagal, Dept of Physics, for sincere assistance with simulation and technical review. This work draws on extensive 5G FR2 research and development, experimental experience within the Microsoft Surface team and studies of radar phased arrays antennas, extended further on 6G sub THz systems research. Also, a big thanks for the opportunities of computational resources MATLAB was used for numerical modeling along with Microsoft Copilot and ChatGPT, Anthropic for language editing, LaTeX formatting and MATLAB debugging.

References

[1] 3GPP TR 38.901, "Study on Channel Model for Frequencies from 0.5 to 100 GHz," v16.1.0, Dec. 2020.
[2] T. S. Rappaport, Y. Xing, O. Kanhere, S. Ju, A. Madanayake, S. Mandal, A. Alkhateeb, and G. C. Trichopoulos, "Wireless Communications and Applications Above 100 GHz: Opportunities and Challenges for 6G and Beyond," *IEEE Access*, vol. 7, pp. 78729–78757, 2019.
[3] Y. Xing and T. S. Rappaport, "Propagation Measurement System and Approach at 140 GHz: Moving to 6G and Above 100 GHz," *arXiv preprint arXiv:1808.07594*, 2019.

[4] S. Ju, Y. Xing, O. Kanhere, and T. S. Rappaport, “Sub-Terahertz Channel Measurements and Characterization in a Factory Building,” *arXiv preprint arXiv:2203.03799*, 2022.

[5] Rohde & Schwarz and IEMN, “Rohde & Schwarz and IEMN collaborate on 6G THz by bringing together electronic and photonic technologies,” press release, 2022.

[6] Rohde & Schwarz, “Rohde & Schwarz drives 6G with sub-THz channel propagation measurements,” press release, European Microwave Week, 2024.

[7] Keysight Technologies Inc., *A New Sub-Terahertz Testbed for 6G Research*, white paper, 2022.

[8] Keysight Technologies Inc., “Keysight Makes UK’s First 100Gbps 6G Sub-THz Connection with National Physical Laboratory and University of Surrey,” press release, Apr. 2023.

[9] Fraunhofer Heinrich-Hertz-Institut, “Terahertz Communication,” Fraunhofer HHI Photonic Networks and Systems Dept., online, accessed 2026.

[10] J. D. Mahony, “A footnote to ‘On the relationship between the directivity and the half power beamwidth in quasi symmetric pencil beam radiation patterns’ [Education Column],” *IEEE Antennas and Propagation Magazine*. https://ieeexplore.ieee.org/document/6387814

[11] Altair Engineering, “Half Power Beamwidth (HPBW),” *Altair WinProp User Guide*, 2021. https://2021.help.altair.com/2021/winprop/topics/winprop/user_guide/aman/introduction/half_power_beamwith_winprop.htm

[12] Keysight Technologies, *N5252B Compact Antenna Test Range Solution Brief*, 2022.

[13] CTIA—The Wireless Association, *Test Plan for Millimeter-Wave Wireless Device Over-the-Air Performance*, v1.0.1, Apr. 2020.

[14] CTIA—The Wireless Association, *Test Plan for Millimeter-Wave Wireless Device Over-the-Air Performance*, v3.8.2, Sept. 2023.